1J3-3

A Fluid-solid Coupled FIT Simulation for Photoacoustic Wave Propagation and Its Experimental Validation

Kazuyuki Nakahata[1†], Miki Akihiro[1], and Taizo Maruyama[1]
([1]Grad. School Sci. Eng., Ehime Univ.)

1.Introduction

Noncontact measurement of the ultrasonic waves using the transmission and reception of laser beam is being introduced in recent nondestructive testing. The ultrasonic wave generated by laser irradiation is called the photoacoustic wave. This is due to the rapid rise of the thermal stress by the laser irradiation, and then the stress wave generates and propagates into the material's interior. The theoretical research and experiment of the photoacoustic effect were conducted intensively in the '80s, and the results were summarized by Scruby and Drain[1)]. Not material parameters related to acoustic, optic, and thermal phenomena, but also spacial and time conditions of the laser irradiation affect the generation of the photoacoustic wave[2)]. Therefore, an appropriate design and preparation are required for reliable laser ultrasonic testing.

Numerical simulation can be an effective tool for predicting photoacoustic signals. This study aims to develop a numerical model to simulate photoacoustic wave generation and propagation. Here, the heat conduction and the elastic wave problems are solved in a coupled manner based on a discretization by the finite integration method[3)] (FIT). In this study, FIT simulations for wavefields with a fluid-solid interface are dealt with, and the accuracy of the method is validated by experimental measurement.

2. Finite Integration Technique

The target area is assumed to be linear elastic solid[s] that satisfy the small-deformation theory. Here, a two-dimensional wave field is considered using the Cartesian coordinates (x_1, x_2). The governing equations of the photoacoustic wave consist of the Cauchy equation of motion and the Duhamel-Neumann's relation[2)]. These equations are given in integral form for a finite volume V with surface S by

$$\int_V \rho \dot{v}_i \mathrm{d}V = \int_S \sigma_{ij} n_j \mathrm{d}S \tag{1}$$

and the Duhamel-Neumann's relation:

$$\int_V \dot{\sigma}_{ij} \mathrm{d}V = \int_S \lambda v_k n_k \delta_{ij} + \mu \left(v_i n_j + v_j n_i \right) \mathrm{d}S - \int_V \left(3\lambda + 2\mu \right) \alpha \delta_{ij} \dot{T} \mathrm{d}V . \tag{2}$$

In Eq.(1), $\boldsymbol{v}(\boldsymbol{x},t)$ is the particle velocity vector, $\boldsymbol{\sigma}(\boldsymbol{x},t)$ is the stress tensor of second-rank, $\rho(\boldsymbol{x})$ is the density, and $\boldsymbol{n}(\boldsymbol{x})$ is the outward normal vector on the surface S. In Eq.(2), $T(\boldsymbol{x},t)$ is the temperature, $\lambda(\boldsymbol{x})$ and $\mu(\boldsymbol{x})$ are the Lame constants, $\alpha(\boldsymbol{x})$ is the linear expansion coefficient, and $\boldsymbol{\delta}$ is the Kronecker delta tensor. In Eqs.(1) and (2), the dot means the derivative in terms of time as $\dot{T} = \partial T / \partial t$, and the summation convention is used.

When modeling the fluid[f], the shear stress $\sigma_{12}(\boldsymbol{x},t) = 0$. By setting $\mu(\boldsymbol{x}) = 0$, we can use a unified grid in both fluid and solid. For the fluid-solid interface, it is essential to satisfy the following continuity conditions

$$v_i^{[\mathrm{f}]}(\boldsymbol{x},t) = v_i^{[\mathrm{s}]}(\boldsymbol{x},t) \tag{3}$$

$$\sigma_{ij}^{[\mathrm{f}]}(\boldsymbol{x},t) = \sigma_{ij}^{[\mathrm{s}]}(\boldsymbol{x},t) = 0 . \tag{4}$$

On the other hand, the heat flux $\boldsymbol{q}(\boldsymbol{x},t)$ and the temperature $T(\boldsymbol{x},t)$ are satisfied by the following the Fourier's law of heat condition:

$$\frac{1}{k} q_i = -\frac{\partial T}{\partial x_i} \tag{5}$$

where k is the thermal conductivity. The equation of heat conduction is expressed using the heat flux as

$$\rho c \dot{T} = -\frac{\partial q_i}{\partial x_i} \tag{6}$$

where c is the specific heat at constant volume.

According to these equations, we perform integration over a cubic voxel V whose surface is S, assuming that $\boldsymbol{v}$, $\boldsymbol{\sigma}$, $\boldsymbol{q}$, and T are constant within V and on S. Here, pixels with a uniform size are used for parallel computation. The length of each side in V is Δx. This method results in staggered grids and

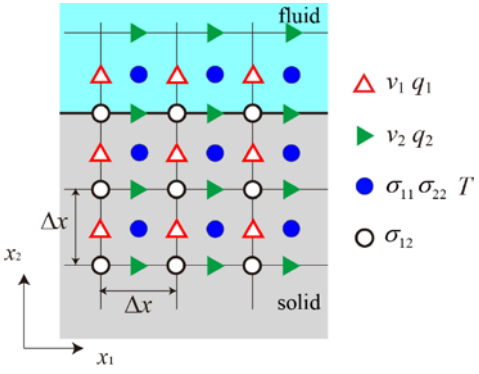

Fig. 1 Finite volume V and the allocation of physical quantities in the 2D FIT.

nakahata@cee.ehime-u.ac.jp

provides a very stable code, allowing easy and flexible treatment of fluid-solid interfacial conditions. The spatial grid of the 2D FIT code is shown in **Fig. 1**.

In the time domain, the stress components ($\boldsymbol{\sigma}$) are allocated at half-time steps, while the velocities (v) and the temperature (T) are allocated at full-time steps. The following time discretization yields an explicit leap-frog scheme:

$$\{\boldsymbol{\sigma}\}^{z+\frac{1}{2}} = \{\boldsymbol{\sigma}\}^{z-\frac{1}{2}} + \Delta t\{\dot{\boldsymbol{\sigma}}\}^{z} \tag{7}$$

$$\{\boldsymbol{v}\}^{z+1} = \{\boldsymbol{v}\}^{z} + \Delta t\{\dot{\boldsymbol{v}}\}^{z+\frac{1}{2}} \tag{8}$$

$$\{T\}^{z+1} = \{T\}^{z} + \Delta t\{\dot{T}\}^{z} \tag{9}$$

where Δt is the time interval, and the superscript z denotes the integer of the time step. The FIT repeats the operations in Eqs.(8),(9), and (10) from $z = 1$ to K under suitable initial and boundary conditions. A specific stability condition[3] (the Courant Friedrichs Lewy condition) and adequate spatial resolution are required to calculate the FIT accurately.

3. Numerical Examples

Simulations of the photoacoustic wave generation and propagation are conducted using two models. One is a solid model (Model A) that consists of aluminum. The other is a two-phase model (Model B) composed of water and aluminum. These material parameters are listed in **Table 1**. Since the photoacoustic effect produced by the absorption of laser is assumed to be prominent on the aluminum surface, we fed the heat flux q_2 on the grids equivalent to the laser spot on the aluminum surface. In the simulation, we set the pulse duration to 7 ns and the laser spot radius to 0.428 mm. The calculation area in Model A is 4mm x 5mm. The pixel size and time incremental in the FIT are 0.5 μm and 0.05 ns, respectively.

The vonMises stresses at 160 ns and 480 ns after the laser irradiation are plotted in **Fig.2**. The magnitude of the stress was normalized by the maximum value for all the time steps in the simulation. From **Fig.2**, the magnitude of the longitudinal (L) wave is smaller than the shear (S) wave. On the other hand, the high intensity of the L wave was observed in Model B (**Fig.3**). By the existence of water, the interface of Model B is subjected to the reaction force in the x_2 direction. Therefore, the amplitude of the normal stress at the interface became large.

Table.1 Material properties of aluminum and water.

Material	Aluminium	Water
Density ρ (kg m^{-3})	2688	996.6
Longitudinal wave velocity c_L (m s^{-1})	6400	1470
Transverse wave velocity c_T (m s^{-1})	3150	–
Linear expansion coefficient α (K^{-1})	2.31×10^{-5}	1.00×10^{-4}
Specific heat c (J kg^{-1} K^{-1})	905	4179
Thermal conductivity k (W m^{-1} K^{-1})	237	0.6104

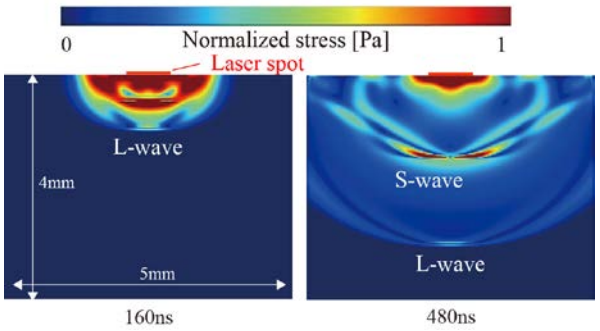

Fig.2 Snapshots of photoacoustic wave propagation in Model A in the case that laser is illuminated on the aluminum surface.

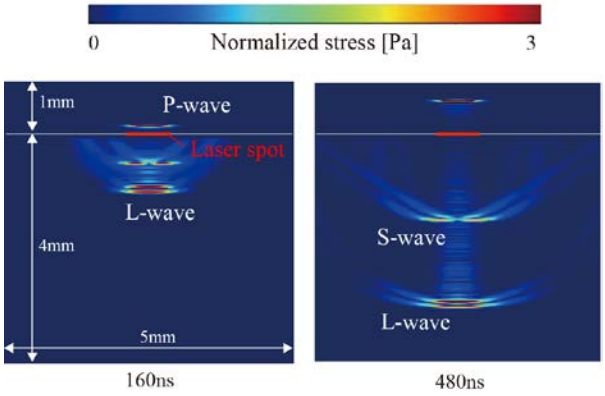

Fig.3 Snapshots of photoacoustic wave propagation in Model B in the case that laser is illuminated on the aluminum surface through the water.

4. Summary

To better understand photoacoustic wave generation and propagation, a numerical simulation method using the discretization of the finite integration technique was proposed. The simulation result showed the photoacoustic wave with large amplitude was observed in the case of the laser irradiation through the water. The experimental results will be shown on the day of the conference.

Acknowledgment

This work was supported by JSPS KAKENHI Grant Number 21H01420JP.

References

1. C. B. Scruby and L. E. Drain: *Ultrasonics, Techniques and Applications* (Adam Hilger, 1990).
2. V. V. Krylov: Ultrasonics, **69** (2016) 279.
3. K. Nakahata, J. Chang, M. Takahashi, K. Ohira and Y. Ogura: Acoust. Sci. Tech. **35**-5 (2014) 260.